

# Binary Constraint Preserving Graph Matching

Bo Jiang<sup>a</sup>, Jin Tang<sup>a</sup>, Chris Ding<sup>b,a</sup>, Bin Luo<sup>a</sup>,

<sup>a</sup>School of Computer Science and Technology, Anhui University, Hefei, 230601, China

<sup>b</sup>CSE Department, University of Texas at Arlington, Arlington, TX 76019, USA

jiangbo@ahu.edu.cn, ahhftang@gmail.com, chqding@uta.edu, luobin@ahu.edu.cn

## Abstract

*Graph matching is a fundamental problem in computer vision and pattern recognition area. In general, it can be formulated as an Integer Quadratic Programming (IQP) problem. Since it is NP-hard, approximate relaxations are required. In this paper, a new graph matching method has been proposed. There are three main contributions of the proposed method: (1) we propose a new graph matching relaxation model, called Binary Constraint Preserving Graph Matching (BPGM), which aims to incorporate the discrete binary mapping constraints more in graph matching relaxation. Our BPGM is motivated by a new observation that the discrete binary constraints in IQP matching problem can be represented (or encoded) exactly by a  $\ell_2$ -norm constraint. (2) An effective projection algorithm has been derived to solve BPGM model. (3) Using BPGM, we propose a path-following strategy to optimize IQP matching problem and thus obtain a desired discrete solution at convergence. Promising experimental results show the effectiveness of the proposed method.*

## 1. Introduction

Many problems in computer vision and pattern recognition can be formulated by graph matching [23, 15, 14, 2, 20, 19]. Recent works [3, 4, 5, 11, 12, 23, 10] have formulated graph matching as an Integer Quadratic Programming (IQP) problem. Since IQP is NP-hard, approximate relaxation methods are required to find approximate solutions for the problem [9, 7, 24, 29, 27, 22].

Many relaxation methods generally aim to optimize the IQP matching problem approximately in a continuous domain. These methods first define a new continuous problem by relaxing the discrete mapping constraint and aim to find the global optimum for the relaxed continuous problem. Then, they use a post-discretization step to obtain the final discrete mapping solution [3, 5, 6]. One limitation for these methods is that the required post-discretization step is generally independent of the matching objective optimiza-

tion which may lead to weak local optimum. Another kind of methods aim to obtain a discrete binary solution for IQP matching problem [12, 28, 1, 16]. For example, Leordeanu et al. [12] proposed an integer projected matching method (IPFP) which optimized the IQP problem directly in a discrete domain and can obtain a discrete binary solution for the problem. Zhou et al. [28, 29] proposed an effective graph matching method (FGM) which optimized the IQP problem approximately using a convex-concave relaxation technique [26] and returns a discrete binary solution for the original problem.

In this paper, we show that the discrete binary constraint in IQP matching problem can be exactly represented (or encoded) by a  $\ell_2$ -norm constraint. Comparing with discrete constraint, the  $\ell_2$ -norm constraint is much easier to implement computationally. To the best of our knowledge, this particular observation has not been explored before, although  $\ell_2$ -norm has been used as a self-amplification regularization term to aid the convergence of the solution to be binary [21]. Based on this new observation, we propose a new graph matching relaxation model, called Binary Constraint Preserving Graph Matching (BPGM), which aims to incorporate the discrete mapping constraints via a  $\ell_2$ -norm constraint in graph matching relaxation. An effective projection algorithm has been developed to solve BPGM model. Moreover, based on BPGM, we propose a path-following strategy to optimize IQP matching problem and thus can obtain a desired discrete solution at convergence. Experimental results on both synthetic and real-world image matching tasks demonstrate the effectiveness of the proposed method.

## 2. Problem Formulation and Related Work

### 2.1. Problem formulation

Given two attributed relation graphs  $G(V, E)$  and  $G'(V', E')$ , each node  $v_i \in V$  or edge  $e_{ik} \in E$  has an attribute vector  $\mathbf{a}_i$  or  $\mathbf{r}_{ik}$  and similarity to  $G'$ . The aim of graph matching problem is to determine the correct correspondence between  $V$  and  $V'$ . Here, we focus on equal-size

graph matching problem. For graphs with different sizes, one can add dummy isolated nodes into the smaller graph and transform them to equal-size case [26, 9]. For each assignment  $(v_i, v'_j)$ , we can define a score  $s_a(\mathbf{a}_i, \mathbf{a}'_j)$  that measures how well node  $v_i \in V$  matches node  $v'_j \in V'$ . Also, for each assignment pair  $(v_i, v'_j)$  and  $(v_k, v'_l)$ , we can define an affinity  $s_r(\mathbf{r}_{ik}, \mathbf{r}'_{jl})$  that measures how compatible the nodes  $(v_i, v_k)$  in  $G$  are with the nodes  $(v'_j, v'_l)$  in  $G'$ . Thus, we can use a matrix  $\mathbf{W}$  in which the diagonal term  $\mathbf{W}_{ij,ij}$  represents  $s_a(\mathbf{a}_i, \mathbf{a}'_j)$ , and the non-diagonal element  $\mathbf{W}_{ij,kl}$  contains  $s_r(\mathbf{r}_{ik}, \mathbf{r}'_{jl})$ . The one-to-one correspondence solution can be denoted by a permutation matrix  $\mathbf{X}$ , i.e.,  $\mathbf{X}_{ij} = 1$  implies that node  $v_i$  in  $G$  corresponds to node  $v'_j$  in  $G'$ , and  $\mathbf{X}_{ij} = 0$  otherwise. In this paper, we denote  $\mathbf{x} = (\mathbf{X}_{11} \dots \mathbf{X}_{1n}, \dots, \mathbf{X}_{n1} \dots \mathbf{X}_{nn})^T$  as a row-wise vectorized replica of  $\mathbf{X}$ . In the following, we call  $\mathbf{X}$  as the matrix form of  $\mathbf{x}$ . The graph matching problem, in its most recent and general form, can be formulated as an Integer Quadratic Programming (IQP) problem [5, 12, 3, 9], i.e.,

$$\max_{\mathbf{x}} \mathbf{x}^T \mathbf{W} \mathbf{x} \quad s.t. \quad \mathbf{A} \mathbf{x} = \mathbf{1}, \mathbf{x}_i \in \{0, 1\} \quad (1)$$

where  $\mathbf{A} \in \{0, 1\}^{(2n) \times n^2}$  is set to encode the doubly stochastic constraint of  $\mathbf{X}$ . It is known that this IQP problem is NP-hard, thus approximate relaxations are required to find approximate solutions for it.

## 2.2. Related work

One popular relaxation way to IQP matching problem Eq.(1) is to relax the binary constraint ( $\mathbf{x}_i \in \{0, 1\}$ ) to the nonnegative domain [4, 28, 11, 5], i.e.,

$$\max_{\mathbf{x}} \mathbf{x}^T \mathbf{W} \mathbf{x} \quad s.t. \quad \mathbf{A} \mathbf{x} = \mathbf{1}, \mathbf{x}_i \geq 0. \quad (2)$$

Since  $\mathbf{W}$  is not necessarily a positive definite matrix, thus this problem Eq.(2) is usually non-convex. Many efforts have been devoted to find the local optimal solution of this relaxation problem [3, 5, 24, 28]. Since the discrete binary constraint has been entirely ignored in this relaxation, the optimal solution is generally continuous and needs to be further binarized to obtain the final discrete binary solution for the original problem Eq.(1) [3, 5]. One drawback is that this abrupt binarization (discretization) step is generally independent of the matching objective optimization and thus may lead to weak local solution for the original problem.

## 3. Binary Preserving Graph Matching

In this section, we propose a new graph matching relaxation model, called Binary Constraint Preserving Graph Matching (BPGM), which aims to incorporate more discrete binary constraint while maintains the affine mapping constraint in matching relaxation. Our BPGM is motivated by a new observation that the discrete constraint  $\mathbf{x}_i \in \{0, 1\}$

in IQP matching problem Eq.(1) can be exactly encoded by a  $\ell_2$ -norm constraint.

### 3.1. BPGM model

By further adding a  $\ell_2$ -norm constraint on the related solution in problem Eq.(2), our BPGM can be formulated as follows,

$$\max_{\mathbf{x}} \mathbf{x}^T \mathbf{W} \mathbf{x} \quad s.t. \quad \mathbf{A} \mathbf{x} = \mathbf{1}, \mathbf{x}_i \geq 0, \|\mathbf{x}\|_2^2 = \gamma, \quad (3)$$

where  $\gamma$  is a parameter and  $\|\mathbf{x}\|_2 = \sqrt{\sum_i \mathbf{x}_i^2}$  is the  $\ell_2$ -norm function. To avoid the conflict between two constraints  $\mathbf{A} \mathbf{x} = \mathbf{1}$  and  $\|\mathbf{x}\|_2^2 = \gamma$ , here  $\gamma$  should satisfy  $\|\mathbf{h}_0\|_2^2 \leq \gamma \leq n$ , where  $\mathbf{h}_0 = \mathbf{A}^T (\mathbf{A} \mathbf{A}^T)^{-1} \mathbf{1}$  and  $n = |V'|$  is the size of graph  $G'$ . This can be seen in detail in §4.2.

One important feature of BPGM model is that it can be viewed as a parameter-controlled **balanced model** between original IQP problem Eq.(1) and its nonnegative relaxation Eq.(2). Thus, it provides a series of parameter-controlled relaxations for IQP matching problem whose tightness are controlled by parameter  $\gamma$ . These can be seen in the following properties in detail.

### 3.2. Properties analysis

**Property 1** When  $\gamma = n$ , BPGM is equivalent to original IQP matching problem Eq.(1).

**Proof.** In BPGM, since  $\mathbf{A} \mathbf{x} = \mathbf{1}, \mathbf{x}_i \geq 0$ , we have

$$\mathbf{x}_i \in [0, 1], \sum_i \mathbf{x}_i = n,$$

where  $n = |V| = |V'|^1$ . Since  $\|\mathbf{x}\|_2^2 = \gamma = n$ , thus, we have  $\sum_i \mathbf{x}_i = \sum_i \mathbf{x}_i^2$ .

That is

$$\sum_i \mathbf{x}_i (1 - \mathbf{x}_i) = 0.$$

Since  $\mathbf{x}_i \geq 0$  and  $0 \leq \mathbf{x}_i \leq 1$ , we have  $\mathbf{x}_i \in \{0, 1\}$ .  $\square$

**Property 2** When  $\gamma = \|\mathbf{x}^*\|_2^2$ , where  $\mathbf{x}^*$  is the optimal solution of relaxed problem Eq.(2), BPGM degenerates to problem Eq.(2).

From Property 1 and 2, we can see that BPGM can be regarded as a balanced model between the relaxed problem Eq.(2) and original problem Eq.(1). This is one important feature of BPGM model. Empirically, the discrete binary level can be controlled by parameter  $\gamma$  in BPGM model, i.e., the larger  $\gamma$ , the more closely  $\mathbf{X}$  (matrix form of  $\mathbf{x}$ ) approximates to a permutation matrix. Figure 1 shows some examples of converged solution  $\mathbf{X}$  under different  $\gamma$  values.

<sup>1</sup>For one-to-one matching problem, the matrix form  $\mathbf{X}$  of  $\mathbf{x}$  is a doubly-stochastic matrix, i.e.,  $\sum_i \mathbf{X}_{ij} = 1, \sum_j \mathbf{X}_{ij} = 1, \mathbf{X}_{ij} \geq 0$ . Thus we have  $\sum_{ij} \mathbf{X}_{ij} = \sum_i \mathbf{x}_i = n$ .

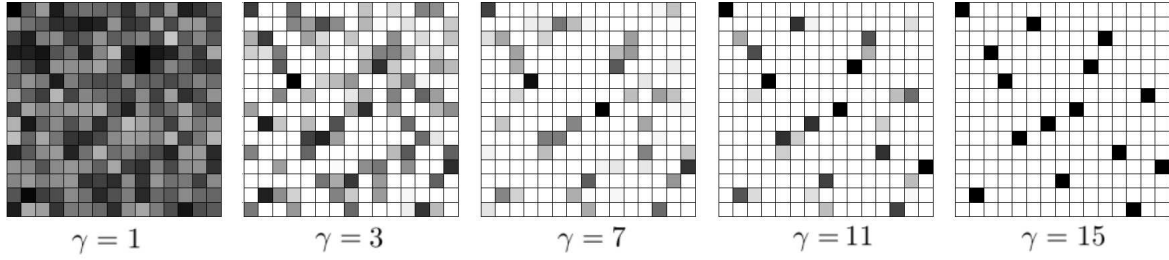


Figure 1. Demonstration of BPGM converged solutions  $\mathbf{X}$  across different  $\gamma$  values ( $|V'| = n = 15$ ).

Here, we can note that, as  $\gamma$  increases, the converged solution becomes more and more sparse. In particular, when  $\gamma = n = 15$ , the converged solution is exactly a permutation matrix.

### 3.3. Path-following strategy

Using BPGM, we can provide a path-following strategy to optimize IQP matching problem (Eq.(1)) which aims to alleviate weak local solution and obtain a better local solution for non-convex problem [28, 26, 16]. In order to do so, we first introduce Lemma 1 which guarantees the good starting point in our path-following process.

**Lemma 1** *There exists a parameter  $\gamma_0$  such that BPGM with  $\gamma = \gamma_0$  has a global optimal solution.*

**Proof.** First, we solve the following problem,

$$\max_{\mathbf{x}} \mathbf{x}^T \mathbf{W}' \mathbf{x} \quad s.t. \quad \mathbf{A}\mathbf{x} = \mathbf{1}, \mathbf{x}_i \geq 0 \quad (4)$$

where  $\mathbf{W}' = \mathbf{W} - \tilde{\mu}_m \mathbf{I}$ ,  $\mathbf{I}$  is a identity matrix, and

$$\tilde{\mu}_m = \begin{cases} 0 & \mu_m < 0 \\ \mu_m + \epsilon & \mu_m \geq 0 \end{cases}$$

where  $\mu_m$  is the maximum eigenvalue of matrix  $\mathbf{W}$  and  $\epsilon > 0$  is a small value. Note that Eq.(4) is convex, thus we can obtain its global optimum  $\tilde{\mathbf{x}}^*$  by using some optimization algorithms, such as Frank-Wolfe algorithm [8]. Then, we set parameter  $\gamma_0$  as

$$\gamma_0 = \|\tilde{\mathbf{x}}^*\|_2^2. \quad (5)$$

Note that,  $\tilde{\mathbf{x}}^*$  is also the global optimum of BPGM model with  $\gamma = \gamma_0$ , i.e., we can obtain the global optimum for BPGM problem with  $\gamma = \gamma_0$ .  $\square$

Based on by Lemma 1 and Property 1, we propose to optimize IQP matching problem by iteratively optimizing a series of the following BPGM problems

$$\max_{\mathbf{x}} \mathbf{x}^T \mathbf{W}\mathbf{x} \quad s.t. \quad \mathbf{A}\mathbf{x} = \mathbf{1}, \mathbf{x}_i \geq 0, \|\mathbf{x}\|_2^2 = \gamma_k \quad (6)$$

where  $k = 0, 1, 2 \dots$  and  $\gamma_0 < \gamma_1 < \dots \leq n$ .

As shown in Lemma 1, when  $\|\mathbf{x}\|_2^2 = \gamma_0$ , the problem has a global optimal solution. When  $\|\mathbf{x}\|_2^2 = n$ , the problem is equivalent to IQP matching problem (Eq.(1)) (Property 1). Our path-following process starts with  $\gamma_0$  and successively tracks a path of solution of a series of BPGM problems with different  $\gamma_k$ , where we solve BPGM problem with  $\gamma_k$  using previous solution  $\mathbf{x}_{\gamma_{k-1}}^*$  as the starting point. By increasing  $\gamma_k$  gradually, the discrete matching constraint can be imposed more and more strongly, and the algorithm can obtain a discrete solution at convergence. For a specific  $\gamma_k$ , we optimize it using the proposed graduated projection algorithm, as shown in §4 in detail. The general schema of our path-following optimization is presented in Algorithm 1. From Property 2, we can note that, in real implement, one can also use the continuous solutions  $\tilde{\mathbf{x}}^*$  of problem Eq.(2) which are obtained from some other methods as the starting point in our BPGM Algorithm 1.

---

#### Algorithm 1 BPGM based path-following algorithm

---

**Input:** Affinity matrix  $\mathbf{W}$ , graph size  $|V| = |V'| = n$ , step size  $\delta$

**Output:** Final discrete matching solution  $\mathbf{x}^*$

- 1: Compute the global optimal solution  $\tilde{\mathbf{x}}^*$  of problem Eq.(4) and set  $\gamma_0 = \|\tilde{\mathbf{x}}^*\|_2^2$
- 2: Initialize  $\mathbf{x}_{\gamma_0}^* = \tilde{\mathbf{x}}^*$ ,  $k = 1$
- 3: **while**  $\gamma_k \leq n$  **do**
- 4: Optimize BPGM model using gradually projection (Eq.(7)) (§4) with initialization  $\mathbf{x}_{\gamma_{k-1}}^*$

$$\mathbf{x}_{\gamma_k}^* = \arg \max_{\mathbf{x}} \mathbf{x}^T \mathbf{W}\mathbf{x} \\ s.t. \quad \mathbf{A}\mathbf{x} = \mathbf{1}, \mathbf{x}_i \geq 0, \|\mathbf{x}\|_2^2 = \gamma_k$$

- 5:  $k = k + 1$
  - 6:  $\gamma_k = \gamma_{k-1} + \delta$
  - 7: **end while**
  - 8:  $\mathbf{x}^* = \mathbf{x}_{\gamma_k}^*$
- 

**Comparison with related works:** Our path-following strategy has some resemblance to the recent popular path-following process used in graph matching [28, 26, 16]. These methods gradually change the objective from convex

to concave formulation to obtain discrete solution. Differently, in our strategy, starting from global solution of the relaxed problem, it gradually changes the constraint from nonnegative domain to discrete domain to obtain the desired discrete solution. Also, the  $\ell_2$  norm constraint has been discussed in the previous work [22]. In work [22], the  $\ell_2$  norm is used to simplify the objective. Differently, we study and use it to encode the discrete constraint and derive a series of relaxation problems.

#### 4. Algorithm

In this section, we design a graduated projection algorithm to solve the proposed BPGM model (Eq.(3)). Let  $J_{gm}(\mathbf{x}) = \mathbf{x}^T \mathbf{W} \mathbf{x}$  and  $\tilde{\lambda}_m$  defined as

$$\tilde{\lambda}_m = \begin{cases} 0 & \lambda_m > 0 \\ |\lambda_m| + \epsilon & \lambda_m \leq 0 \end{cases}$$

where  $\lambda_m$  is the minimum eigenvalue of affinity matrix  $\mathbf{W}$ . Here,  $\tilde{\lambda}_m$  is set to make matrix  $\tilde{\mathbf{W}} = \mathbf{W} + \tilde{\lambda}_m \mathbf{I}$  positive definite. The proposed algorithm updates the current solution  $\mathbf{x}^k$  by iteratively solving the following projection problem,

$$\begin{aligned} \mathbf{x}^{k+1} &= \arg \min_{\mathbf{v}} \|\mathbf{v} - \tilde{\mathbf{W}} \mathbf{x}^k\|_2^2 \\ \text{s.t. } \mathbf{A} \mathbf{v} &= \mathbf{1}, \|\mathbf{v}\|_2^2 = \gamma, \mathbf{v}_i \geq 0. \end{aligned} \quad (7)$$

The iteration starts with an initial  $\mathbf{x}^0$  and is repeated until convergence.

From algorithm aspect, this projection process has some resemblance to the work [25]. Differently, we further consider the nonnegative constraints  $\mathbf{v}_i \geq 0$ . This nonnegative constraints  $\mathbf{v}_i \geq 0$  along with affine constraint  $\mathbf{A} \mathbf{v} = \mathbf{1}$  are necessary for encoding the discrete binary constraint in BPGM model, as discussed in §3.2. In the following, we first present the convergence property of this update algorithm, and then provide the detail computation of this projection problem.

#### 4.1. Convergence analysis

**Theorem 1** *Under the update projection Eq.(7), the graph matching objective function  $J_{gm} = \mathbf{x}^T \mathbf{W} \mathbf{x}$  is monotonically increasing.*

**Proof.** Similar to the proof of work [25], problem Eq.(7) is equivalent to

$$\begin{aligned} \mathbf{x}^{k+1} &= \arg \max_{\mathbf{v}} \mathbf{v}^T \mathbf{u}^k = \arg \max_{\mathbf{v}} \mathbf{v}^T \tilde{\mathbf{W}} \mathbf{x}^k \\ \text{s.t. } \mathbf{A} \mathbf{v} &= \mathbf{1}, \|\mathbf{v}\|_2^2 = \gamma, \mathbf{v}_i \geq 0. \end{aligned} \quad (8)$$

This implies

$$\mathbf{x}^{k+1 T} \tilde{\mathbf{W}} \mathbf{x}^k > \mathbf{x}^k T \tilde{\mathbf{W}} \mathbf{x}^k. \quad (9)$$

Also, since  $\tilde{\mathbf{W}}$  is a positive definite matrix, we have

$$\begin{aligned} &\mathbf{x}^{k+1 T} \tilde{\mathbf{W}} \mathbf{x}^{k+1} + \mathbf{x}^k T \tilde{\mathbf{W}} \mathbf{x}^k - 2 \mathbf{x}^{k+1 T} \tilde{\mathbf{W}} \mathbf{x}^k \\ &= (\mathbf{x}^{k+1} - \mathbf{x}^k)^T \tilde{\mathbf{W}} (\mathbf{x}^{k+1} - \mathbf{x}^k) > 0. \end{aligned} \quad (10)$$

Combing inequality Eq.(9) and Eq.(10), we conclude that  $\mathbf{x}^{k+1 T} \tilde{\mathbf{W}} \mathbf{x}^{k+1} > \mathbf{x}^k T \tilde{\mathbf{W}} \mathbf{x}^k$ . That is,

$$\mathbf{x}^{k+1 T} (\mathbf{W} + \tilde{\lambda}_m \mathbf{I}) \mathbf{x}^{k+1} > \mathbf{x}^k T (\mathbf{W} + \tilde{\lambda}_m \mathbf{I}) \mathbf{x}^k. \quad (11)$$

Note that  $\mathbf{x}^{k+1 T} \mathbf{x}^{k+1} = \|\mathbf{x}^{k+1}\|_2^2 = \|\mathbf{x}^k\|_2^2 = \mathbf{x}^k T \mathbf{x}^k = \gamma$ , thus we have

$$\mathbf{x}^{k+1 T} \mathbf{W} \mathbf{x}^{k+1} > \mathbf{x}^k T \mathbf{W} \mathbf{x}^k. \quad (12)$$

This completes the proof.

#### 4.2. Constraint projection

Here we solve the projection problem Eq.(7). We rewrite problem Eq.(7) as

$$\min_{\mathbf{v}} \|\mathbf{v} - \mathbf{u}\|_2^2 \quad \text{s.t. } \mathbf{A} \mathbf{v} = \mathbf{1}, \|\mathbf{v}\|_2^2 = \gamma, \mathbf{v}_i \geq 0 \quad (13)$$

where  $\mathbf{u} = \tilde{\mathbf{W}} \mathbf{x}^k$ . We will use the Von-Neumann successive projection method [17] to solve this problem. In order to do so, we first define the following two sub-projections, i.e., the affine sub-projection

$$P_1(\mathbf{v}) = \arg \min_{\mathbf{v}} \|\mathbf{v} - \mathbf{u}\|_2^2 \quad \text{s.t. } \mathbf{A} \mathbf{v} = \mathbf{1}, \|\mathbf{v}\|_2^2 = \gamma, \quad (14)$$

and the convex sub-projection

$$P_2(\mathbf{v}) = \arg \min_{\mathbf{v}} \|\mathbf{v} - \mathbf{u}\|_2^2 \quad \text{s.t. } \mathbf{v}_i \geq 0. \quad (15)$$

The process of Von-Neumann method [17] is to alternatively conducts sub-projection  $P_1$  and  $P_2$  until convergence to obtain the optimal solution for constraint projection problem Eq.(13).

In the following, we show that both problem  $P_1$  and  $P_2$  have closed-form solution and thus can be solved efficiently. For problem  $P_1$ , similar projection has been proposed in work [25]. Here, we concerns a more general case, i.e.,  $\|\mathbf{v}\|_2^2 = \gamma$ . Similar to work [25], we have the following,

**Lemma 2** *Problem  $P_1$  has a closed-form optimal solution. The optimal solution  $\mathbf{v}^*$  is*

$$\mathbf{v}^* = \sqrt{\gamma - \|\mathbf{h}_0\|_2^2} \frac{\mathbf{P} \mathbf{u}}{\|\mathbf{P} \mathbf{u}\|_2} + \mathbf{h}_0, \quad (16)$$

where  $\mathbf{P} = \mathbf{I} - \mathbf{A}^T (\mathbf{A} \mathbf{A}^T)^{-1} \mathbf{A}$ ,  $\mathbf{h}_0 = \mathbf{A}^T (\mathbf{A} \mathbf{A}^T)^{-1} \mathbf{1}$ .

**Proof.** Indeed, the problem  $P_1$  is equivalent to

$$P_1(\mathbf{v}) = \arg \max_{\mathbf{v}} \mathbf{v}^T \mathbf{u} \quad s.t. \quad \mathbf{A}\mathbf{v} = \mathbf{1}, \|\mathbf{v}\|_2 = \gamma. \quad (17)$$

First, it is easy to see that  $\tilde{\mathbf{v}} = \frac{\sqrt{\gamma - \|\mathbf{h}_0\|_2^2} \mathbf{P}\mathbf{u}}{\|\mathbf{P}\mathbf{u}\|_2}$  is the normalized projection of  $\mathbf{u}$  onto the intersection space  $\mathbf{A}\mathbf{v} = \mathbf{0}$  and  $\|\tilde{\mathbf{v}}\|_2 = \gamma - \|\mathbf{h}_0\|_2^2$ . Thus,  $\tilde{\mathbf{v}}$  is the optimal solution of the problem,

$$\tilde{\mathbf{v}} = \arg \max_{\mathbf{v}} \mathbf{v}^T \mathbf{u} \quad s.t. \quad \mathbf{A}\mathbf{v} = \mathbf{0}, \|\mathbf{v}\|_2 = \gamma - \|\mathbf{h}_0\|_2^2 \quad (18)$$

Then, we can infer that  $\mathbf{v}^* = \tilde{\mathbf{v}} + \mathbf{h}_0$  is the optimal solution of problem Eq.(17), as shown in work [25]. Also, we can see that the parameter  $\gamma$  should to satisfy  $\gamma \geq \|\mathbf{h}_0\|_2^2$ , as discussed before.  $\square$

**Lemma 3** Problem  $P_2$  has a closed-form optimal solution. The optimal solution  $\mathbf{v}^*$  is

$$\mathbf{v}^* = \frac{1}{2}(\mathbf{u} + |\mathbf{u}|). \quad (19)$$

### 4.3. Computational complexity

The main computational complexity in each iteration of the algorithm is on computing  $\mathbf{W}\mathbf{x}^k$  and solving the projection problem Eq.(13). Thus, the computational complexity for each iteration is less than  $O(n^2) + O(Nn^2)$ , where  $N$  is average number of iterations on solving problem Eq.(13). Empirically, the algorithm converges quickly and the average number of iterations  $N$  is generally less than 150.

## 5. Experiments

In this section, we have applied our BPGM method to the matching tasks including synthetic graph matching, feature point matching using image sequences and feature matching on real-world images. We have compared our BPGM method with some other state-of-the-art methods including SM [11], IPFP [12], SMAC [5], RRWM [3] and FGM [28]. We implemented IPFP with two versions: (1) IPFP-U that is initialized by the uniform solution; (2) IPFP-S that is initialized by SM [11].

### 5.1. Synthetic graph matching

Our first experiment is based on synthetic random graph data. Following the experimental setting [3], we first generated two random graphs,  $G$  and  $G'$ , both of them contain  $n_{in}$  inlier nodes. Then we added  $n_{out}$  outlier nodes in both graphs. For each pair of nodes in  $G$ , the edge is randomly generated according to the density  $\rho \in [0, 1]$ . For each edge in  $G$ , we assigned a random attribute  $\mathbf{r}_{ij}$  which is uniformly distributed from 0 to 1. The corresponding edge  $\mathbf{r}'_{i'j'}$  in  $G'$  was perturbed by adding a random Gaussian type perturbation noise  $N(0, \sigma)$  to the value of  $\mathbf{r}_{ij}$ . For each noise level  $\sigma$

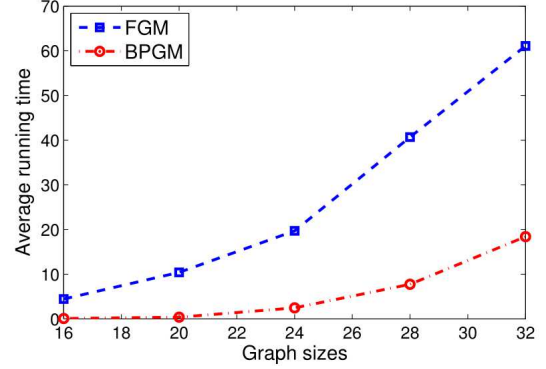


Figure 3. Comparison results on running times.

or  $n_{out}$ , we have generated 100 random graph pairs and then computed the average performances including matching accuracy and objective score. The matching accuracy is measured by the number of detected true matches divided by the total number of ground truths, and the objective score is computed by  $\mathbf{x}^T \mathbf{W}\mathbf{x}$  of the IQP objective. The affinity matrix  $\mathbf{W}$  is computed by  $\mathbf{W}_{ij,kl} = \exp(-(\mathbf{r}_{ik} - \mathbf{r}'_{jl})^2 / 0.015)$ . Figure 2 summarizes the comparison results on matching accuracy and objective score. As discussed before, compared with RRWM [3], the main feature of our BPGM is that it incorporates more the discrete binary constraint in optimization process. From Figure 2, we can note that BPGM consistently returns higher objective score and matching accuracy than RRWM [3] method, which clearly demonstrates the benefits of discrete constraint in searching for the optimal solution for IQP matching problem. BPGM outperforms the discrete domain projection method IPFP [12], indicating that BPGM can find a discrete solution more optimal than IPFP method. Also, BPGM performs slightly better than FGM [28], which demonstrates the effectiveness and robustness of BPGM method.

Our BPGM iteratively solves a series of problems using Path-following strategy and thus slower than some other single optimization algorithms such as RRWM [3], SM [11] and IPFP [12]. However, it is generally faster than previous path-following algorithm. Figure 3 shows comparison of running times between FGM [28] and BPGM. We can note that, BPGM is faster than FGM [28].

### 5.2. Feature point matching across image sequence

Our second experiment is performed on feature matching tasks on CMU "hotel" sequence dataset [2, 3]. For this dataset, there are 101 images of a toy house captured from moving viewpoints. For each image, there exist about 30 landmark points which were manually marked with known correspondences. For each image, the coordinates of these landmark points were normalized to  $[0, 1]$ . We have matched all images spaced by 5, 10, 15  $\dots$  75 and 95 frames and computed the average accuracy per sep-

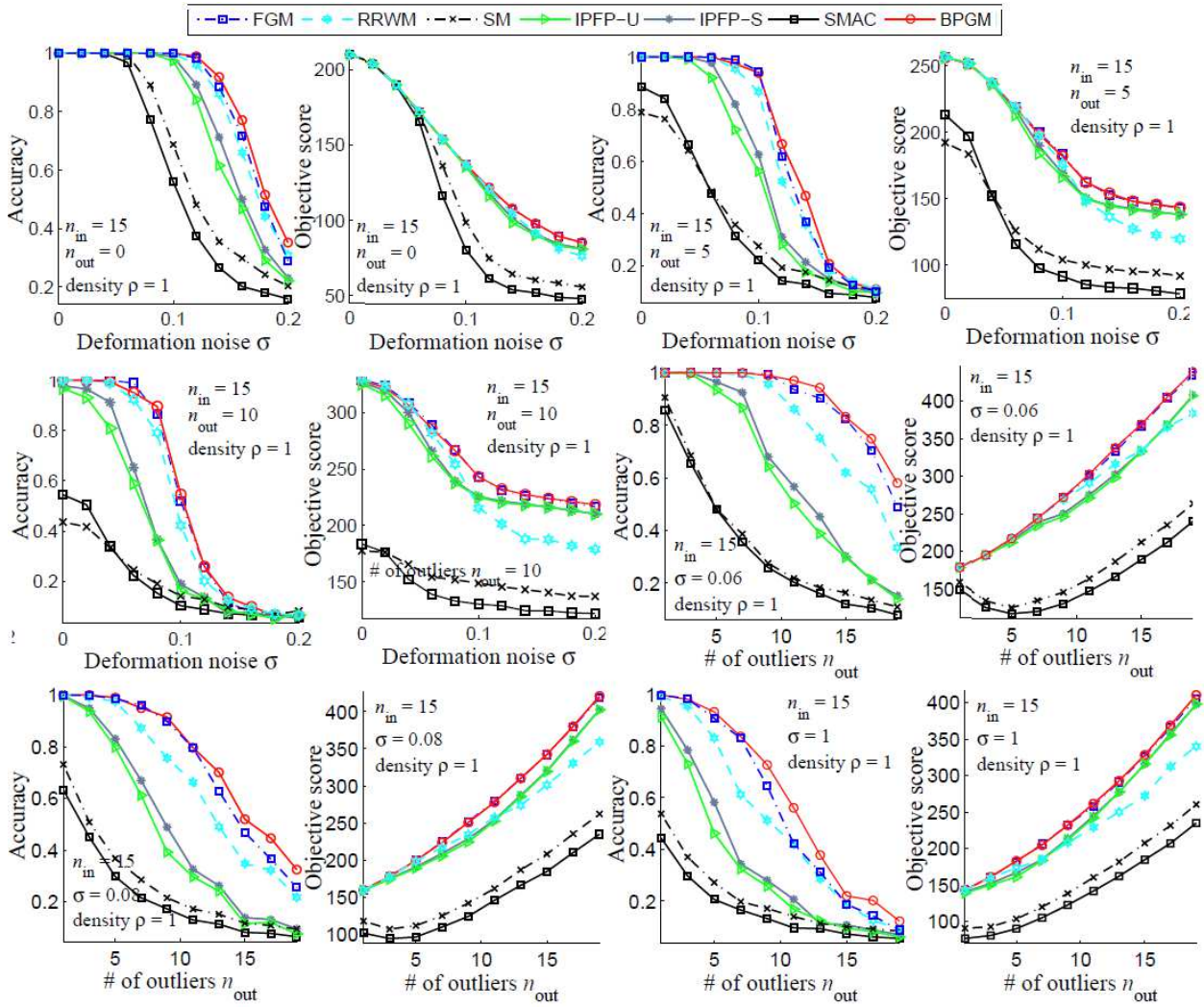


Figure 2. Comparison results on synthetic graph matching.

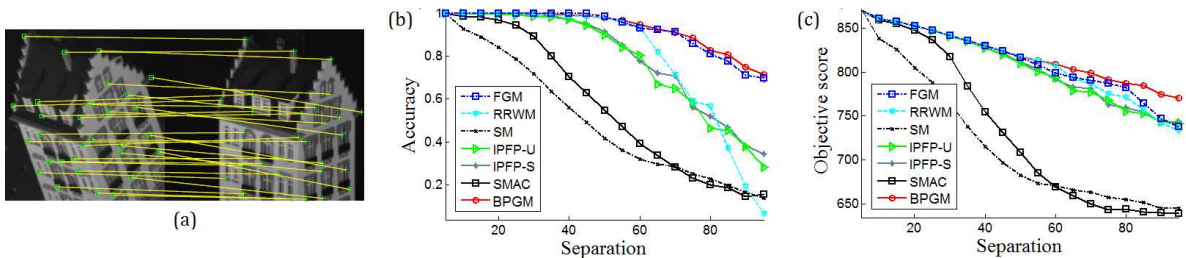


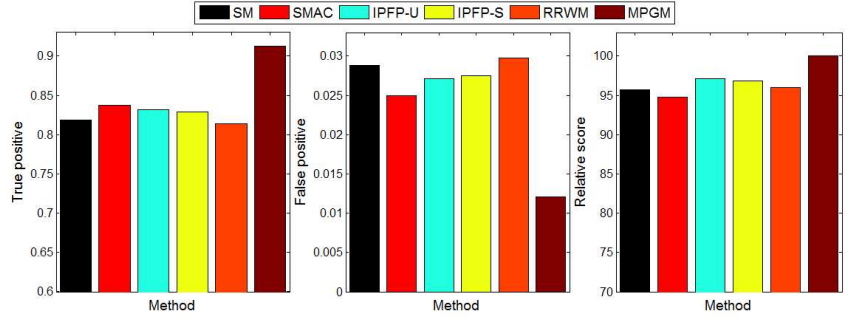
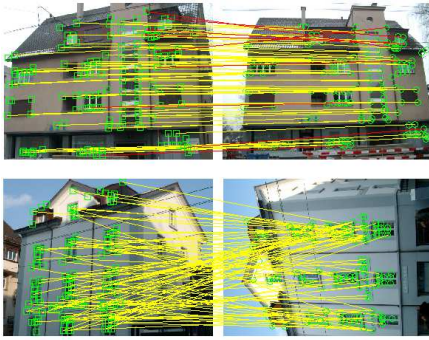
Figure 4. Comparison results on CMU image sequence.

eration gap. For each image pair, the affinity matrix has been computed by  $\mathbf{W}_{ij,kl} = \exp(-(\mathbf{r}_{ik} - \mathbf{r}'_{jl})^2 / 0.015)$ , where  $\mathbf{r}_{ik}$  is the Euclidean distance between two points. Figure 4 summarizes the performance results with respect to the separation gaps on CMU image sequence dataset. It is noted that BPGM outperforms the other methods in both matching accuracy and objective score. This is generally consistent

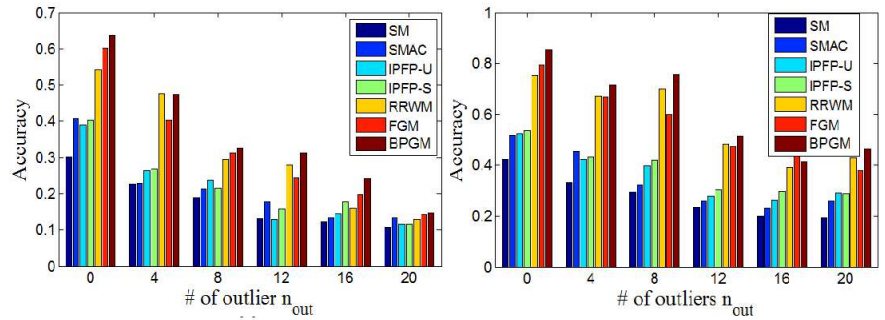
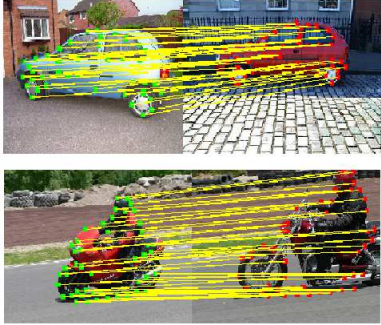
with the results on the synthetic data experiments and further demonstrates the effectiveness of the proposed BPGM method.

### 5.3. Real-world image matching

In this experiment, we first evaluate our BPGM method on the image pairs (30 pairs) selected from Zurich Build-



(a) ZuBud image dataset



(b) Pascal dataset

Figure 5. Comparison results on real-world image datasets.

ing Image Database (ZuBud) [18]. The candidate correspondences have been generated using the SIFT descriptor. Here, each feature in first image can match the six closest features in the second image using the distance of SIFT descriptor. The affinity between two correspondences has been computed as  $\mathbf{W}_{ij,kl} = \exp(-(d_{ik} - d_{jl})^2/1500)$ , where  $d_{ik}$  is the Euclidean distance between the feature points  $i$  and  $k$ , and similar to  $d_{jl}$ . For all image pairs in this dataset, the average performances including true positive and false positive and relative objective score [3] are computed. We compare our method with SM, SMAC, IPFP and RRWM, because FGM method cannot be directly used here. Figure 5 (a) shows the comparison results. Note that BPGM obtains better performance than other compared methods on true positive, false positive and objective score, which demonstrates the effectiveness and optimality of BPGM method on solving real-world image feature matching problem. Then, we test our matching method on the Pascal image dataset which consists of 30 pairs of car images and 20 pairs of motorbike images selected from Pascal 2007 dataset [13, 28]. Each pair contains 30-60 ground-truth correspondences. The coordinates of the feature point were first normalized to  $[0, 1]$ . Here, we generated complete graphs and each edge was assigned by the Euclidean distance between two nodes. The affinity between two correspondences was computed as  $\mathbf{W}_{ij,kl} =$

$\exp((\mathbf{r}_{ik} - \mathbf{r}'_{jl})^2/0.015)$ , where  $\mathbf{r}_{ik}, \mathbf{r}'_{jl}$  are the Euclidean distances between two points. Figure 5 (b) summarizes the comparison results. BPGM generally performs better than other compared methods, which further demonstrates the effectiveness of BPGM method on conducting real-world image feature matching tasks.

## 6. Conclusions

In this paper, we first propose a new graph matching relaxation model, called Binary Constraint Preserving Graph Matching (BPGM), which incorporates the discrete binary mapping constraints via a  $\ell_2$  norm constraint. BPGM can be regarded as a parameter-controlled balanced model between the original IQP matching problem Eq.(1) and its nonnegative relaxation Eq.(2). An effective projection algorithm has been developed to solve the proposed BPGM model. The convergence of the algorithm is theoretically guaranteed. Based on BPGM, we also provide a new path-following process to optimize IQP matching problem. Promising experimental results on several matching tasks show the effectiveness and benefits of the proposed method.

Note that the path-following strategy and algorithm proposed in this paper are not limited to graph matching problem only and can also be used in some other similar problems, such as MAP inference.

## Acknowledgment

This work is supported by the National Key Basic Research Program of China (973 Program) (2015CB351705); National Natural Science Foundation of China (61602001,61472002,61671018); Natural Science Foundation of Anhui Province (1708085QF139); Natural Science Foundation of Anhui Higher Education Institutions of China (KJ2016A020); The Open Projects Program of National Laboratory of Pattern Recognition.

## References

- [1] K. Adamczewski, Y. Suh, and K. M. Lee. Discrete tabu search for graph matching. In *ICCV*, pages 109–117, 2015.
- [2] T. S. Caetano, J. J. McAuley, L. Cheng, Q. V. Le, and A. J. Smola. Learning graph matching. *PAMI*, 31(6):1048–1058, 2009.
- [3] M. Cho, J. Lee, and K. M. Lee. Reweighted random walks for graph matching. In *ECCV*, pages 492–505, 2010.
- [4] D. Conte, P. Foggia, C. Sansone, and M. Vento. Thirty years of graph matching in pattern recognition. *IJPRAI*, pages 265–298, 2004.
- [5] M. Cour, P. Srinivasan, and J. Shi. Balanced graph matching. In *NIPS*, pages 313–320, 2006.
- [6] A. Egozi, Y. Keller, and H. Guterman. A probabilistic approach to spectral graph matching. *PAMI*, 35(1):18–27, 2013.
- [7] O. Enqvist, K. Josephson, and F. Kahl. Optimal correspondences from pairwise constraints. In *ICCV*, pages 1295–1302, 2009.
- [8] M. Frank and P. Wolfe. An algorithm for quadratic programming. *Naval Research Logistics Quarterly*, 3(1-2):95–110, 1956.
- [9] S. Gold and A. Rangarajan. A graduated assignment algorithm for graph matching. *PAMI*, 18(4):377–388, 1996.
- [10] B. Jiang, J. Tang, and B. Luo. Attributed relational graph matching with sparse relaxation and bistochastic normalization. In *GbrPR*, pages 218–227, 2015.
- [11] M. Leordeanu and M. Hebert. A spectral technique for correspondence problem using pairwise constraints. In *ICCV*, pages 1482–1489, 2005.
- [12] M. Leordeanu, M. Hebert, and R. Sukthankar. An integer projected fixed point method for graph matching and map inference. In *NIPS*, pages 1114–1122, 2009.
- [13] M. Leordeanu, R. Sukthankar, and M. Hebert. Unsupervised learning for graph matching. *Int. J. Comput. Vis.*, 95(1):1–18, 2011.
- [14] L. Lin, K. Zeng, X. B. Liu, and S. C. Zhu. Layered graph matching by composite cluster sample with collaborative and competitive interactions. In *CVPR*, pages 1351–1358, 2009.
- [15] H. Ling and D. W. Jacobs. Shape classification using inner-distance. *PAMI*, 29(2):286–299, 2007.
- [16] Z. Y. Liu and H. Qiao. Gncpp-graduated nonconvexity and concavity procedure. *PAMI*, 36(6):1258–1267, 2014.
- [17] J. V. Neumann, editor. *Functional Operators (Vol. II)*. Princeton University, 1950.
- [18] E. S. Ng and N. G. Kingsbury. Matching of interest point groups with pairwise spatial constraints. In *ICIP*, pages 2693–2696, 2010.
- [19] Q. N. Ngoc, A. Gautier, and M. Hein. A flexible tensor block coordinate ascent scheme for hypergraph matching. In *CVPR*, pages 5270–5278, 2015.
- [20] Q. Nguyen, F. Tudisco, A. Gautier, and M. Hein. An efficient multilinear optimization framework for hypergraph matching. *PAMI*, 2016.
- [21] M. Pelillo. Replicator equations, maximal cliques, and graph isomorphism. *Neural Computation*, 11:1933–1955, 1999.
- [22] Y. Tian, J. Yan, H. Zhang, Y. Zhang, X. Yang, and H. Zha. On the convergence of graph matching: Graduated assignment revisited. In *ECCV*, pages 821–835. Springer, 2012.
- [23] L. Torresani, V. Kolmogorov, and C. Rother. Feature correspondence via graph matching: Models and global optimization. In *ECCV*, pages 596–609, 2008.
- [24] B. J. van Wyk and M. A. van Wyk. A pocs-based graph matching algorithm. *PAMI*, 16(11):1526–1530, 2004.
- [25] L. Xu, W. Li, and D. Schuurmans. Fast normalized cut with linear constraints. In *CVPR*, pages 2866–2873, 2009.
- [26] M. Zaslavskiy, F. Bach, and J. P. Vert. A path following algorithm for the graph matching problem. *PAMI*, 31(12):2227–2242, 2009.
- [27] Z. Zhang, Q. Shi, J. McAuley, W. Wei, Y. Zhang, and A. V. D. Hengel. Pairwise matching through max-weight bipartite belief propagation. In *CVPR*, pages 1202–1210, 2016.
- [28] F. Zhou and F. D. la Torre. Factorized graph matching. In *CVPR*, pages 127–134, 2012.
- [29] F. Zhou and F. D. la Torre. Deformable graph matching. In *CVPR*, pages 127–134, 2013.